DISCONTINUOUS BOUNDARY CONDITION IMPACT ON NEAR CORNER STRESS VALUES AROUND A SPHERICAL CAVITY

AHMADREZA HABIBI
Norwegian University of Science and Technology, Norway

ABSTRACT
Numerical solutions for solid mechanics problems with a rapid variation of quantities in a small domain may result in impractical estimates. The presence of a cavity in an elastic domain, as a classic example, enforces more complexity on a large model due to its stress concentration impact. Boundary element method (BEM) as a numerical method applicable to this type of problem, also involves singular kernels. Due to the implementation complexity of augmented integration schemes, there is still a tendency to use ordinary integration techniques. Besides, enforcing boundary conditions might also be challenging in BEM. In this study, near-corner stress values are explored to evaluate the impact of straightforward integration schemes and discontinuous boundary enforcement treatments. Provided results demonstrate that for coordinates near corners in this specific problem, using non-conforming elements and shape functions with displacement vectors might reduce the error values to fewer than 1%. Further, despite the results for nodes away from corners, unique traction can compromise accuracy for near-corner coordinates in exchange for its simple implementation.
Keywords: boundary element method, non-conforming elements, corner points.

1 INTRODUCTION

Incorporating analytical solutions, boundary element method (BEM) has the capacity to provide precise results for a problem with high field variable gradients. Considerably, BEM weaknesses regarding computer memory and processing speed have been improved using computing algorithms, larger built-in memory, and parallel codes; however, the presence of challenges like singular integrands and corner points still might be problematic [1]–[6].

The traction vector in applied BEM formulation has been derived using the analytical solution for displacement and elasticity theory; therefore, it is dependent on the normal vectors of the boundary surface, and it causes difficulties in implementation for discontinuous boundary conditions and corner points. Among many suggested methods to address the issue, rounding off the boundary, extra degrees of freedom [1], [7], [8], unique traction [9], [10], additional collocation points [5], [11], [12], non-conforming elements (applied here) [2], [13]–[18] can be mentioned.

In the present work, elastostatic BEM code results have been evaluated for a problem with stress concentration. A classic problem with a high gradient of field variables and an available analytical solution is the spherical cavity inside an elastic solid [19], [20]. In previous research outputs [9], [21], using the same problem, the accumulated stress error values away from the corners have been presented. In this study, the error values near corners have been calculated separately for each internal position for different non-conforming elements, mesh, and integration points by employing simple integration and approximation methods.

2 GOVERNING EQUATIONS AND METHODS

The basic BEM formulation is mentioned in eqn (1).

$$C_{ij}u_j(P) = \int_{\Gamma} U_{ij}(Q,P)\, t_j(Q)\, d\Gamma(Q) - \oint_{\Gamma} T_{ij}(Q,P)\, u_j(Q)\, d\Gamma(Q). \qquad (1)$$

www.witpress.com, ISSN 1743-3533 (on-line)
doi:10.2495/BE470031

Terms U and T are well-known singular functions from Kelvin's solution, Γ is the boundary surface, and the second integral on the right sight of the equations implies that the Cauchy principal value is applied. Moreover, δ_{ij}, u, and t are the Kronecker delta function, displacement, and traction variables, respectively. Also, P and Q represent source and field points [1], [3]. As free term (C_{ij}) can not be calculated easily using direct methods, widely utilised free rigid body motion has been used [22]; this also provides accurate diagonal arrays of the matrix T.

The only augmented integration scheme used in this study is the degenerate mapping of a triangle to a standard quadrilateral element which has a zero Jacobian of mapping [1], [23]. This approach was applied for coordinates close to an element surface (critical distance was set to a few times more than the largest element length [24]). For coordinates close to an element, division to triangles and degenerate mapping were done using the closet position on the element. Moreover, results of this study have been derived by 6 and 12 Gaussian quadrature in each direction.

To tackle the discontinuous boundary conditions, unique tractions (UT), semi-discontinuous element (SDE), improved semi-discontinuous element (SDEI), and discontinuous element (DE) have been used separately. While UT considers a unique traction vector as the variable and enforces extra specified traction boundary conditions using a separate constant vector, other methods generate new nodes at specific locations and introduce new degrees of freedom to differentiate between variables where it is mathematically required. Elaborating, DE displaces all nodes even if one of them has discontinuous traction values. The only difference between SDE and SDEI is that in SDEI, if it is possible, nodes are moved along the edges rather than into the element surface. Therefore, for all methods, the integration surface is similar, while nodal positions are different [21].

Stress error calculation was performed using an analytical solution provided and utilised for a cavity inside an infinite elastic domain [19]–[21]. By choosing a proper model size, the solution result can be applied for finite domain. Further, error value was derived using relative error equation for each coordinate separately. As the simple integration scheme applied here cannot tackle the strong singularity for nodes near the boundary, in the post-processing section, nodal positions of hexahedral elements for stress and subsequently error calculation were considered; this allowed the program to use shape functions and the BEM stress equation as two different ways of stress calculation.

3 NUMERICAL RESULTS

Using a similar model to previous works [9], [21], a cavity inside a cubic elastic body was considered. Benefiting from the symmetrical feature of the problem, 1/8 of the model was designed to be meshed and imported as the imported data file. The cube side length was big enough to avoid the boundary effect around the cavity. A tensile surface force of 1 MN on top (positive Z-direction) and proper boundary conditions on other surfaces were enforced (see Fig. 1). Two sets of hexahedral elements, so close to corners, were considered for post-processing; the stress values for their nodes were calculated with both the BEM solution and shape functions and compared with the analytical solution to produce error values for each coordinate separately (see Fig. 1 and Table 1).

4 RESULTS AND DISCUSSION

Stress error value results have been depicted in Fig. 3. Due to the high error values at some cases and coordinates, all error values more than an acceptable value (1%) are shown by one

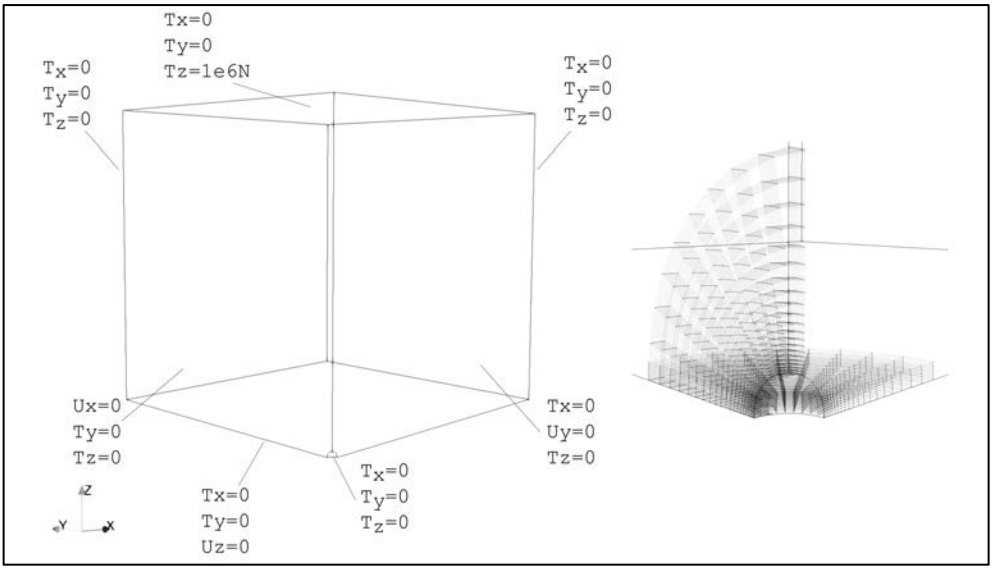

Figure 1: An outline of the model and boundary conditions (left) and post-processing elements' nodal (right).

Table 1: Analysis input data.

Material properties	Young's modulus (Pa)	Poisson's ratio		
	1.00E+09	0.3		
BEM mesh	Element length (m)			
	Cavity surface	Lateral surface		
1	~0.18	0.2<L<0.28		
2	~0.09	0.1<L<0.18		
Post-processing sets	Set position and distance to the boundary		Distance ratio to the BEM element length	
	Parallel to boundary plane/ off-set (m)	Distance to the cavity surface (m)	Cavity element s	Parallel boundary surface elements
1	X–Y plane/0.02	0.02	~0.11	~0.1
2	Y–Z plane/0.02	0.02	~0.22	~0.2

colour, which is a sign of computation method failure (applied to all figures). Therefore, this comparison is focused on the error values lower than 1%. Also, DE and SDEI results were not included in the figure due to the similarity to SDE results. Furthermore, Fig. 2 illustrates different nodal coordinates in various methods. Worth mentioning that despite previous work [9], this study is more focused on separated error values for coordinates near corners.

Due to the simple integration scheme, the BEM stress equation deviated from the solution at the nodes close to the boundary. However, noticeably, high error values were mostly at the

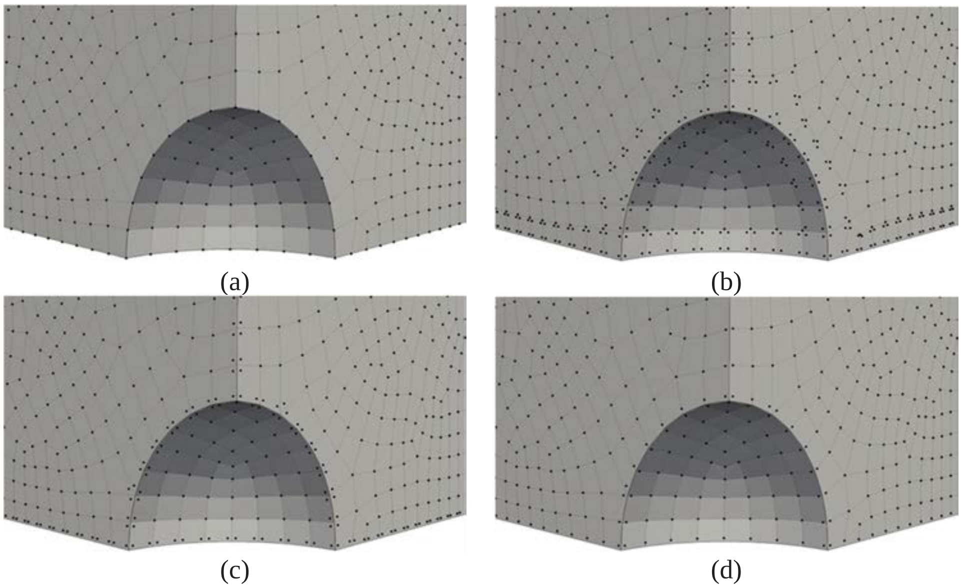

Figure 2: Different nodal positions in (a) UT, (b) DE, (c) SDE, and (d) SDEI.

first layer of nodes, while the distance between the two closest layers to the boundary is 0.05 m, which implies that boundary layer impact has disappeared at a few fractions of element length. Moreover, refining the mesh to half the size has provided minor improvements for the BEM equation and slightly better results for nodes near the cavity at the bottom face (see for example Fig. 3(b) and (f)).

Interestingly, using shape functions in UT for both meshes provided inaccurate stress values near corners and more precise values for nodes along the boundaries away from corners (see Fig. 3(a) and (e)). When non-conforming elements were utilised, hexahedral shape functions provided more accurate results at nearly all nodal coordinates for both meshes (see Fig. 3(c)). However, none of the approaches eliminated the errors for the BEM stress formulation raised due to integration (see Fig. 3(b), (d), and (f)).

All non-conforming elements' results were regenerated with two higher deviation ratio constants (ratio of the distance at which nodes were displaced to make non-conforming elements) for both meshes. The comparison of accumulated error values suggested that the change in error values was quite negligible. However, for stress values calculated using shape functions, compared to the other two methods, there was a slightly more consistent increase trend in SDEI error values by increasing the degree of discontinuity (see Fig. 4). Additionally, a more quantitative comparison showed that although the accumulated error values of the non-conforming methods were so close, the highest point-wise error values limit for SDE and SDEI, calculated using shape functions, were slightly lower than DE.

Furthermore, simulations were reprocessed by increasing the number of Gaussian quadrature points from six to 12 in each direction. The results indicated slight improvement in error values calculated using shape functions. However, for the BEM formulation, a noticeable reduction in error values was observed for coordinates near the boundaries. Interestingly, the degree of improvement was less pronounced for the coarse mesh, likely due

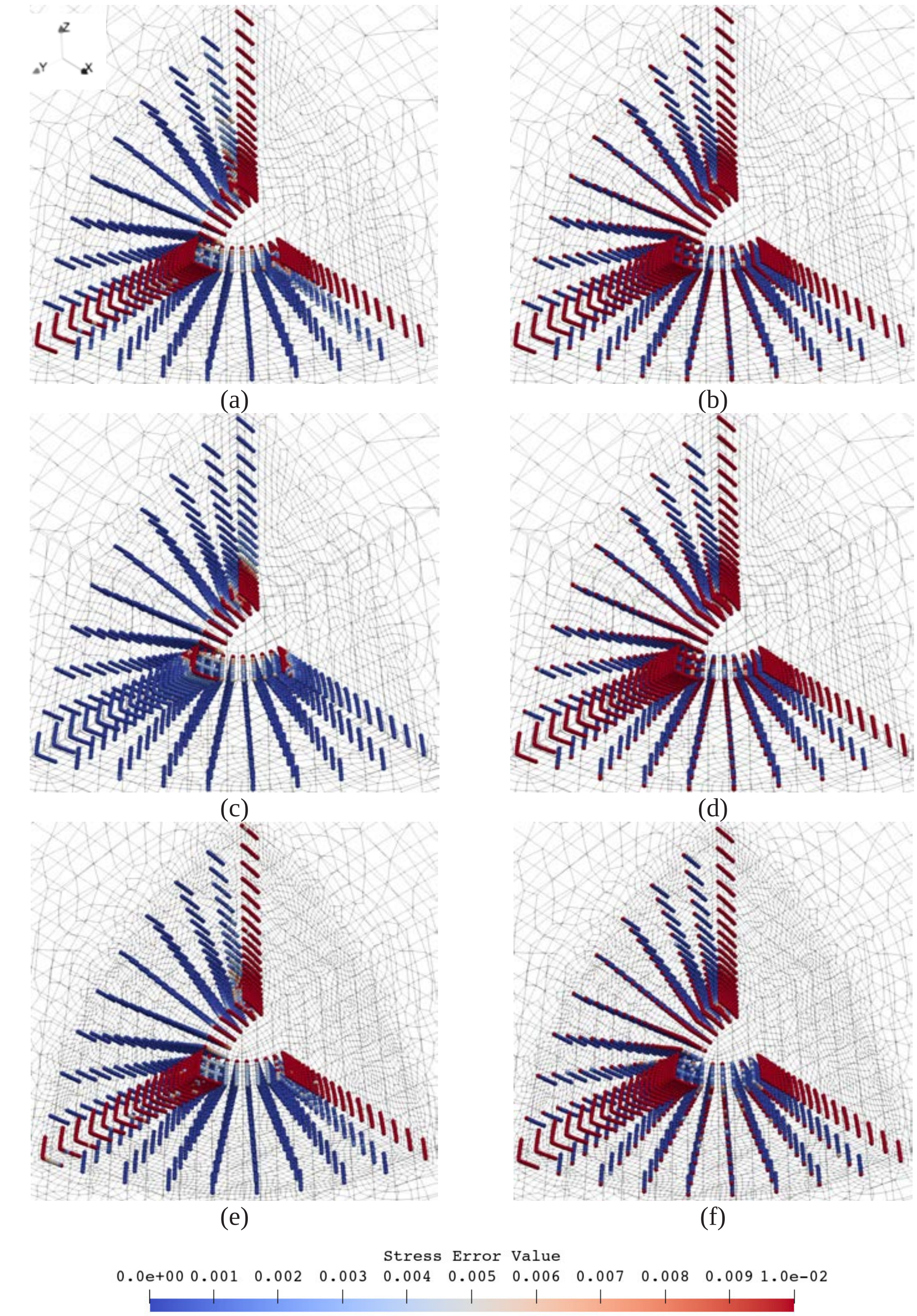

Figure 3: Nodal error values of stress tensor calculated in post-processing using element shape functions (left panel) and the BEM stress formula (right panel) for both coarse and fine meshes. (a) UT-coarse mesh; (b) UT-coarse mesh; (c) SDE-coarse mesh; (d) SDE-coarse mesh; (e) UT-fine mesh; and (f) UT-fine mesh.

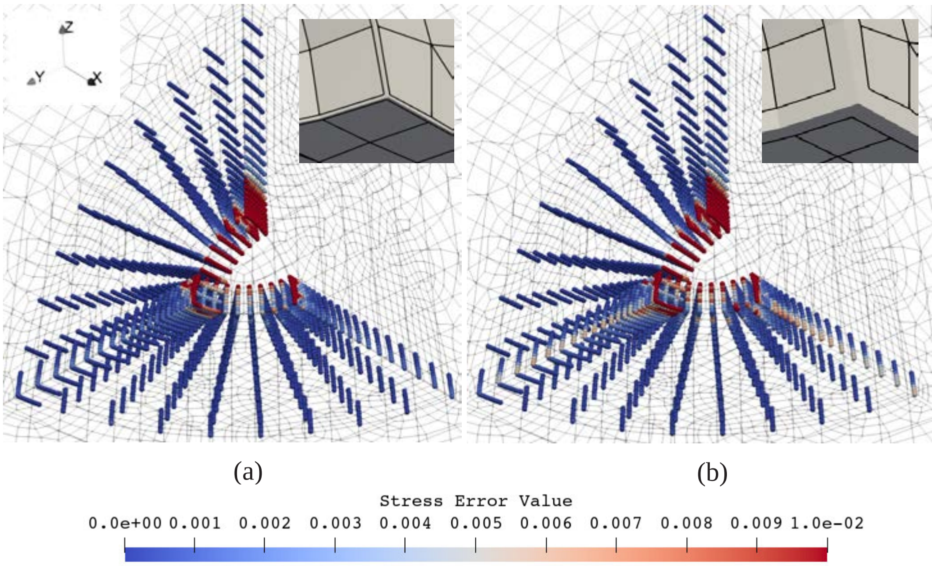

Figure 4: Stress error values calculated using shape functions and SDEI elements with higher deviation ratio in (b).

to the stronger boundary layer effect associated with bigger elements (see Fig. 5). To further reduce the boundary layer effects, the model was meshed with 0.05 m elements. Despite this refinement, still for some coordinates close to the boundary (0.02 m distance) high BEM formula error values were detected (Fig. 6). Thus, increasing the number of collocation and integration points without adequately addressing higher-order BEM stress formula singularities in this range of distance ratios may not eliminate the risk of erroneous results.

5 CONCLUDING REMARKS

In this study, the impact of the boundary layer and non-conforming elements on the accuracy of discontinuous traction vectors and stress function singularity was examined.

Based on the results provided using an elastostatic BEM code, it was shown that for this specific problem, non-conforming elements can yield accurate results when post-processing coordinates are placed near corners. Furthermore, even with simple integration schemes, the BEM stress equation can still deliver accurate results for coordinates just a few element-length fractions away from the boundary. These findings align with the previous research outputs on coordinates away from corners.

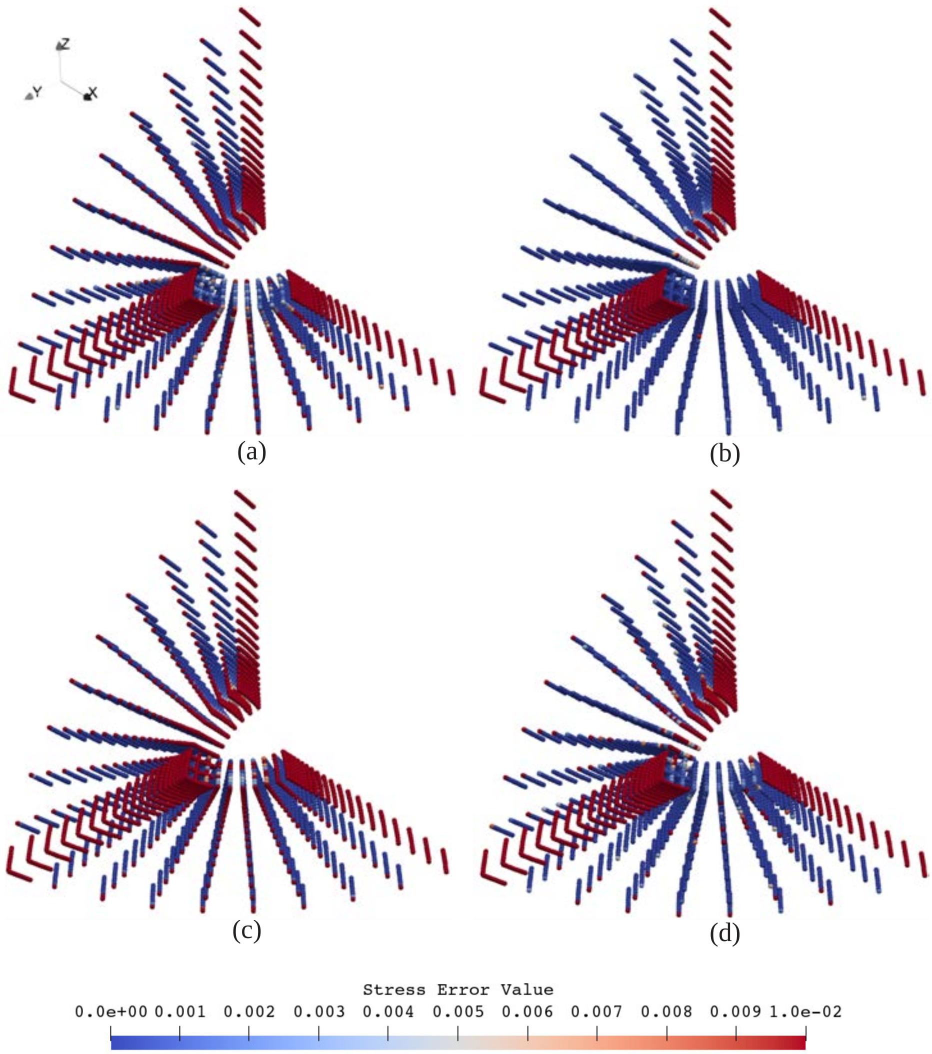

Figure 5: Change in BEM formula stress error values with an increase in the number of Gaussian quadrature points from six (left panel) to 12 (right panel). (a) and (b) show results for the fine mesh; (c) and (d) show the results for the coarse mesh.

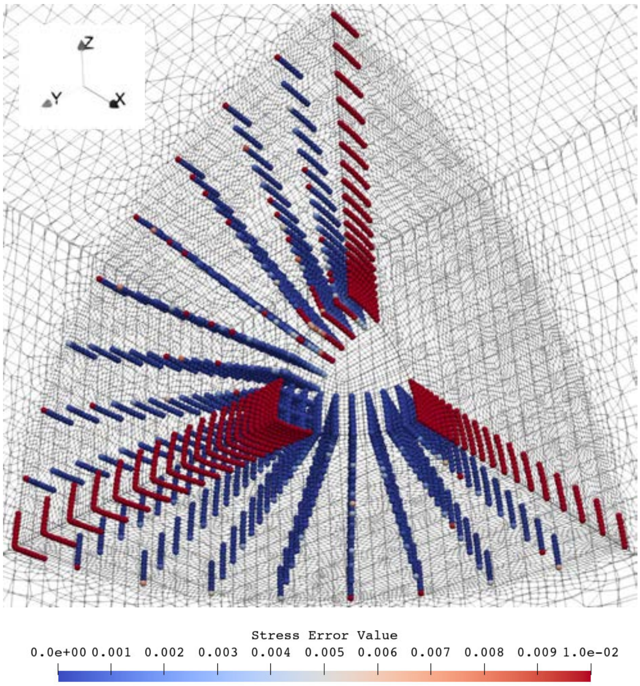

Figure 6: BEM stress formulation error values for SDE method and an element size of 0.05 m in the vicinity of the cavity.

REFERENCES

[1] Gao, X.-W. & Davies, T.G., *Boundary Element Programming in Mechanics*, Cambridge University Press, 2002.

[2] Aliabadi, M.H., *The Boundary Element Method, Volume 2: Applications in Solids and Structures*, Wiley, 2002.

[3] Crouch, S.L., Starfield, A.M. & Rizzo, F., *Boundary Element Methods in Solid Mechanics*, 1983.

[4] Alarcon, E., Brebbia, C. & Dominguez, J., The boundary element method in elasticity. *International Journal of Mechanical Sciences*, **20**(9), pp. 625–639, 1978.

[5] Leng, D., *Boundary Element Method in Anisotropic Media with Grain Sliding and Dislocation Dynamics*, Iowa State University, 2007.

[6] Hall, W.S., Boundary element method. *The Boundary Element Method*, Springer, pp. 61–83, 1994.

[7] Gao, X.-W. & Davies, T., 3D multi-region BEM with corners and edges. *International journal of Solids and Structures*, **37**(11), pp. 1549–1560, 2000.

[8] Qin, X., Lei, W., Li, H. & Fan, Y., Corner treatment in 3D time-domain boundary element method. *Journal of the Brazilian Society of Mechanical Sciences and Engineering*, **44**(11), p. 556, 2022.

[9] Habibi, A., Numerical stress computation around cavity using boundary element method for elastic material. *58th US Rock Mechanics/Geomechanics Symposium*, 2024.

[10] Cruse, T.A., An improved boundary-integral equation method for three dimensional elastic stress analysis. *Computers and Structures*, **4**(4), pp. 741–754, 1974.
[11] Mitra, A.K. & Ingber, M.S., A multiple-node method to resolve the difficulties in the boundary integral equation method caused by corners and discontinuous boundary conditions. *International Journal for Numerical Methods in Engineering*, **36**(10), pp. 1735–1746, 1993.
[12] Wang, Z. & Wu, Q., A new approach treating corners in boundary element method. *Boundary Elements XIII*, Springer, pp. 901–911, 1991.
[13] Dyka, C. & Millwater, H., Formulation and integration of continuous and discontinuous quadratic boundary elements for two dimensional potential and elastostatics. *Computers and Structures*, **31**(4), pp. 495–504, 1989.
[14] Yan, G. & Lin, F.-B., Treatment of corner node problems and its singularity. *Engineering Analysis with Boundary Elements*, **13**(1), pp. 75–81, 1994.
[15] Mi, Y. & Aliabadi, M., Dual boundary element method for three-dimensional fracture mechanics analysis. *Engineering Analysis with Boundary Elements*, **10**(2), pp. 161–171, 1992.
[16] Parreira, P., On the accuracy of continuous and discontinuous boundary elements. *Engineering Analysis*, **5**(4), pp. 205–211, 1988.
[17] Okada, H., Rajiyah, H. & Atluri, S.N., A novel displacement gradient boundary element method for elastic stress analysis with high accuracy, 1988.
[18] Manolis, G. & Banerjee, P., Conforming versus non-conforming boundary elements in three-dimensional elastostatics. *International Journal for Numerical Methods in Engineering*, **23**(10), pp. 1885–1904, 1986.
[19] Neuber, H., *Theory of Notch Stresses: Principles for Exact Stress Calculation*, JW Edwards, 1946.
[20] Brethauer, G. (ed.), Stress around pressurized spherical cavities in triaxial stress fields. *International Journal of Rock Mechanics and Mining Sciences and Geomechanics Abstracts*, Elsevier, 1974.
[21] Habibi, A., Comparison of boundary element numerical techniques for corner point treatment. Submitted for publication.
[22] Brebbia, C.A., Telles, J.C.F. & Wrobel, L.C., *Boundary Element Techniques: Theory and Applications in Engineering*, Springer Science and Business Media, 2012.
[23] Lean, M.H. & Wexler, A., Accurate numerical integration of singular boundary element kernels over boundaries with curvature. *International Journal for Numerical Methods in Engineering*, **21**(2), pp. 211–228, 1985.
[24] Telles, J., A self-adaptive co-ordinate transformation for efficient numerical evaluation of general boundary element integrals. *International Journal for Numerical Methods in Engineering*, **24**(5), pp. 959–973, 1987.